

## Research Article

# Preparation and Characterization of Silver Nanoparticles-Loaded Calcium Alginate Beads Embedded in Gelatin Scaffolds

Porntipa Pankongadisak,<sup>1</sup> Uracha Rungsardthong Ruktanonchai,<sup>2</sup> Pitt Supaphol,<sup>3</sup> and Orawan Suwanton<sup>1,4</sup>

Received 6 January 2014; accepted 24 April 2014; published online 23 May 2014

**Abstract.** Silver nanoparticles (AgNPs)-loaded alginate beads embedded in gelatin scaffolds were successfully prepared. The AgNPs-loaded calcium alginate beads were prepared by electrospraying method. The effect of alginate concentration and applied voltage on shape and diameter of beads was studied. The diameter of dry AgNPs-loaded calcium alginate beads at various concentrations of AgNO<sub>3</sub> ranged between 154 and 171 μm. The AgNPs-loaded calcium alginate beads embedded in gelatin scaffolds were fabricated by freeze-drying method. The water swelling and weight loss behaviors of the AgNPs-loaded alginate beads embedded in gelatin scaffolds increased with an increase in the submersion time. Moreover, the genipin-cross-linked gelatin scaffolds were proven to be nontoxic to normal human dermal fibroblasts, suggesting their potential uses as wound dressings.

**KEY WORDS:** alginate beads; electrospraying; gelatin; scaffolds; silver nanoparticles.

## INTRODUCTION

Metal nanoparticles, produced from silver, gold, and copper, have been reported and well known for their antibacterial properties. Silver nanoparticles (AgNPs) are widely used as antibacterial agents due to their nontoxicity and strong antibacterial activity (1). AgNPs can be synthesized by chemical reduction using sodium borohydride (NaBH<sub>4</sub>), formamide, and triethanolamine. The advantages of this method are its simplicity and effectiveness. However, its disadvantages such as biological toxicity and environmental hazard of residual reducing agents have been reported. Other methods such as X-ray irradiation, UV irradiation, and microwave were also used to synthesize AgNPs since they can eliminate the purification step for removing the residual reducing agents (2).

Electrohydrodynamic spraying or electrospraying is a technique that has been reported to produce polymer beads for controlled release (3–5). It is a process of liquid atomization with electrical forces. In this process, the liquid flowing out from a capillary nozzle which is maintained at high electric potential is applied by the electric field to be dispersed into

droplets (6). The size of droplets can be varied from hundreds micrometers down to tens nanometers. The shape and size of droplets can be controlled by the flow rate of the liquid and the voltage at the capillary nozzle (7). Recently, several parameters affecting the shape of alginate beads produced by electrospraying/extrusion were studied. The results showed that higher voltage, higher calcium chloride concentration, shorter width of electrical field, and slower extrusion rates resulted in small size of alginate beads (8). Moreover, bovine serum albumin (BSA) was used as a protein model drug and loaded in the alginate beads by electrospraying method. The results showed that the higher amount of initial BSA and the slower releasing rate of BSA from the formulation were observed (9).

Alginate is a natural polysaccharide extracted from brown seaweed. It is composed of β-D-mannuronic acid (M) and α-L-guluronic acid (G) (10). It is cross-linked with calcium ions to form gel, known as “the egg-box model” (11,12). Generally, it can be used as living cell encapsulant matrices (13), wound dressings (14), and intranasal drug delivery devices (15). In addition, it can encapsulate angiogenic growth factors, such as basic fibroblast growth factor (bFGF) and the vascular endothelial growth factor (VEGF) to treat ischemia.

Polymeric scaffolds are substrates for the implanted cells with good physical support to control the tissue restoration or improve the functional tissue regeneration (16). In addition, the polymeric scaffolds can support cell adhesion, migration, proliferation, and differentiation (17). Scaffolds should have three-dimensional architecture, highly porous with a large surface area/volume ratio, and well-interconnected open pore structure. Moreover, they should be mechanically strong, malleable, biocompatible, and biodegradable (18–20). Freeze-drying used to produce the polymeric scaffolds involves the formation of ice crystals inside polymer solution during

**Electronic supplementary material** The online version of this article (doi:10.1208/s12249-014-0140-9) contains supplementary material, which is available to authorized users.

<sup>1</sup> School of Science, Mae Fah Luang University, Tasud, Muang, Chiang Rai 57100, Thailand.

<sup>2</sup> National Nanotechnology Center, Thailand Science Park, Klong Luang, Pathumthani 12120, Thailand.

<sup>3</sup> The Petroleum and Petrochemical College and The Center of Excellence on Petrochemical and Materials, Chulalongkorn University, Pathumwan, Bangkok 10330, Thailand.

<sup>4</sup> To whom correspondence should be addressed. (e-mail: o.suwanton@gmail.com)

freezing, and those ice crystals act as porogen particles during lyophilization, resulting in the forming of a porous three-dimensional polymeric scaffolds (21). Gelatin is widely used in medical applications as scaffold materials because of its biocompatibility, low immunogenicity, and biodegradability (22).

The aim of this work is to develop a method for controlling and sustaining release of AgNPs from the AgNPs-loaded calcium alginate beads embedded in gelatin scaffolds. The effect of alginate concentration and the applied voltage on the morphology and size of the calcium alginate beads was studied. The calcium alginate beads incorporated with AgNPs were obtained by electro spraying method. UV irradiation technique was used to reduce the silver ( $\text{Ag}^+$ ) ions in alginate solution to AgNPs. Moreover, The AgNPs-loaded calcium alginate beads embedded in gelatin scaffolds were fabricated by freeze-drying method. The shape and size of both the neat and the AgNPs-loaded calcium alginate beads were observed by optical microscope (OM) and scanning electron microscope (SEM). The morphological appearance of both neat and the AgNPs-loaded calcium alginate beads embedded in gelatin scaffolds was also studied. The water swelling and weight loss behaviors of the AgNPs-loaded calcium alginate beads embedded in gelatin scaffolds were investigated. Lastly, the indirect cytotoxicity of the genipin-cross-linked gelatin scaffolds with different genipin concentrations was investigated.

## EXPERIMENTAL DETAILS

### Materials

Gelatin (type A, porcine skin, ~180 Bloom) was purchased from Fluka Analytical (Switzerland). Genipin powder (98% purity) was obtained from Shanghai Angoal Chemical (China). Sodium alginate was purchased from Carlo Erba (Italy). Silver nitrate ( $\text{AgNO}_3$ ;  $\geq 99.9\%$  purity) was purchased from Fisher Scientific (USA). Calcium chloride ( $\text{CaCl}_2$ ), sodium chloride, anhydrous disodium hydrogen orthophosphate, and sodium dihydrogen orthophosphate (Ajax Chemicals,

Australia) were analytical reagent grade and used without further purification.

### Preparation of Both Neat and AgNPs-Loaded Calcium Alginate Beads

Firstly, the optimal condition for producing calcium alginate beads was carried out by electro spraying method (Fig. 1). The concentration of sodium alginate solution was 0.5, 1.0, and 1.5% *w/v*, and the applied voltage was 8, 10, 12, and 15 kV. The prepared sodium alginate solutions were then extruded dropwise through a needle placed into a glass syringe capped with a 24-gauge blunt needle (an internal diameter of needle is 0.55 mm) into a 0.5-M  $\text{CaCl}_2$  solution under an applied electric field. The distance between tip to collector was fixed at 15 cm. The calcium alginate beads were collected in  $\text{CaCl}_2$  solution with gentle stirring for 30 min. The obtained calcium alginate beads were washed with deionized water and then lyophilized for 20 h.

For the AgNPs-loaded calcium alginate beads, the preparation was presented in Fig. 2. The base sodium alginate solution was prepared at a fixed concentration of 1.5% *w/v*. The AgNPs-loaded sodium alginate solutions were prepared by adding 1, 2, and 3% *w/w*  $\text{AgNO}_3$  (based on the weight of sodium alginate) into the base sodium alginate solutions. According to the previous method (23), the  $\text{Ag}^+$  ions in the alginate solution was reduced to AgNPs by UV irradiation at 254 nm for 1 h. Prior to electro spraying, the solutions were characterized for their viscosity and conductivity at room temperature ( $26 \pm 1^\circ\text{C}$ ) using a Brookfield/RVDV-II+P viscometer and a CyberScan con 200 conductivity meter, respectively. These solutions were then extruded dropwise through a needle into a 0.5-M  $\text{CaCl}_2$  solution under a fixed electric field of 12 kV/15 cm using the electro spraying method. The obtained AgNPs-loaded calcium alginate beads were left in the  $\text{CaCl}_2$  solution for 30 min. Finally, these beads were separated from  $\text{CaCl}_2$  solution and then washed with deionized water. It should be noted that the calcium alginate beads containing 1, 2, and 3% *w/w* of  $\text{AgNO}_3$  are hereafter

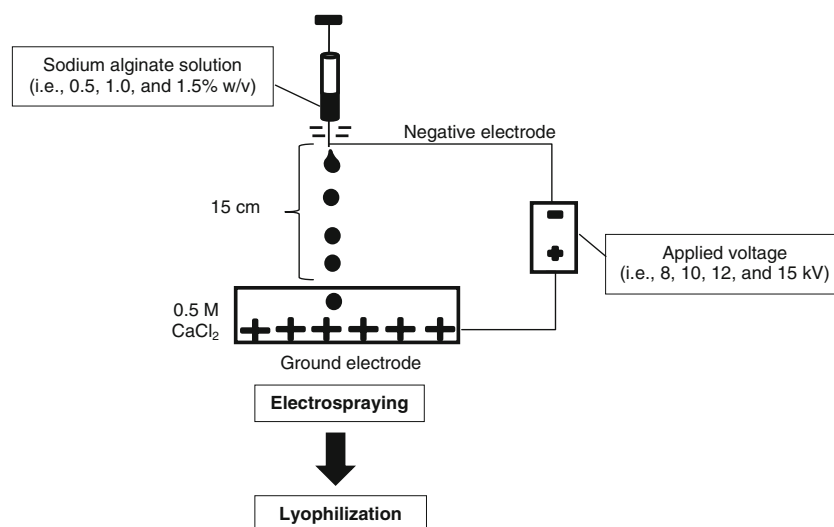


**Fig. 1.** Scheme preparation of calcium alginate beads by electro spraying method

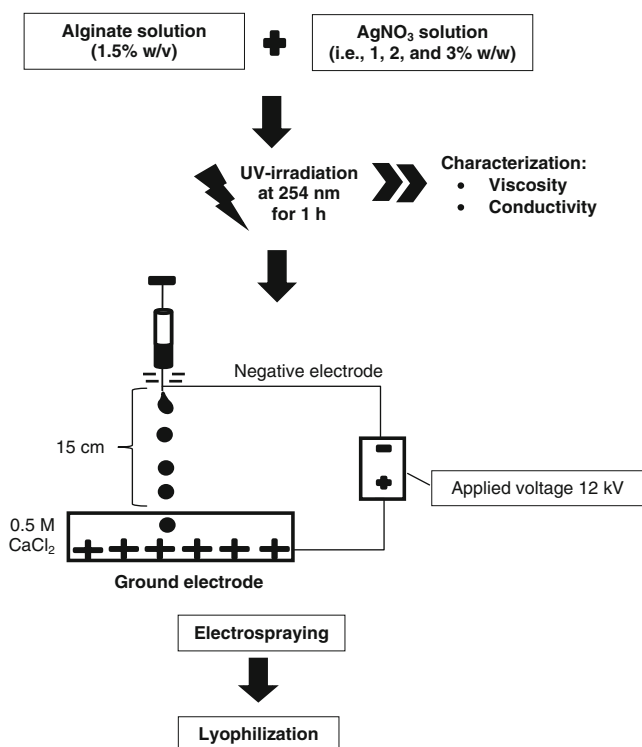


**Fig. 2.** Scheme preparation of AgNPs-loaded calcium alginate beads by electrospaying method

denoted as 1, 2, and 3% AgNPs-loaded calcium alginate beads, respectively.

### Preparation of Genipin-Cross-linked Gelatin Scaffolds and AgNPs-Loaded Calcium Alginate Beads Embedded in Gelatin Scaffolds

Gelatin powder was dissolved in boiled deionized water to prepare the base gelatin solution at a fixed concentration of 5% *w/v*. Genipin was used as a cross-linking agent to cross-link the amino acid groups of gelatin as shown in Fig. 3 (24). Various concentrations of genipin (*i.e.*, 3, 4, 5, and 6% *w/w* based on the weight of gelatin powder) were added into gelatin solutions, and then, the solutions were stirred at room temperature for 1 h. These solutions were then poured into polypropylene (PP) mold and lyophilized to form scaffolds by freeze-drying method.

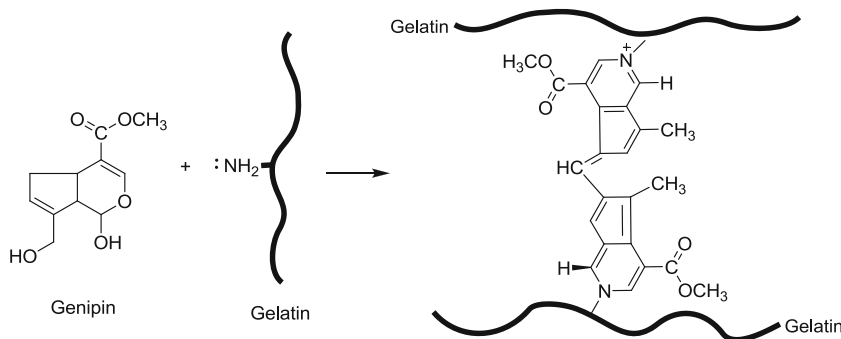


**Fig. 3.** Schematic illustration of the intermolecular cross-linking structures of genipin with gelatin

The dry 1, 2, and 3% AgNPs-loaded calcium alginate beads were used to embed in the gelatin scaffolds. The AgNPs-loaded calcium alginate beads embedded in gelatin scaffolds were prepared by adding 1% *w/w* of the AgNPs-loaded calcium alginate beads (based on the weight of gelatin powder) into 5% *w/v* of gelatin solutions. These solutions were then poured into PP mold and cross-linked at room temperature for 24 h. The AgNPs-loaded calcium alginate beads embedded in gelatin scaffolds were obtained by lyophilization.

### Morphological Observation

The shape and size of both the neat and the AgNP-loaded calcium alginate beads were investigated by Motic BA300 optical microscope (OM) using the magnification of 4 $\times$  and a LEO 1450 VP scanning electron microscope (SEM). For the morphological observation, each sample was coated with a thin layer of gold using a Polaron SC-7620 sputtering device. The diameters of the beads were measured directly from OM and SEM images using a Motic Images Plus 2.0 and a SemAphore 4.0 software, respectively.

The shape and size of AgNPs in the AgNPs-loaded calcium alginate beads were investigated by a JEOL JEM-2100 transmission electron microscope (TEM). The dispersion of the AgNPs-loaded calcium alginate beads in ethanol solution was placed on carbon-coated copper grid. The sample grid was kept in desiccator cabinet until the solvent was slowly evaporated.

The genipin-cross-linked gelatin scaffolds and the AgNPs-loaded calcium alginate beads embedded in the gelatin scaffolds were characterized for their morphological appearance by SEM. Each sample was coated with a thin layer of gold using a Polaron SC-7620 sputtering device prior to the observation under SEM. Pore sizes of the scaffolds were measured directly from SEM images using a SemAphore 4.0 software. More than 30 pores of each sample group were measured.

### Indirect Cytotoxicity Evaluation of Genipin-Cross-linked Gelatin Scaffolds

The indirect cytotoxicity evaluation of genipin-cross-linked gelatin scaffolds was conducted in adaptation from the ISO 10993-5 standard test method in a 96-well tissue-culture polystyrene plate (TCPS; Corning Costar®, USA)

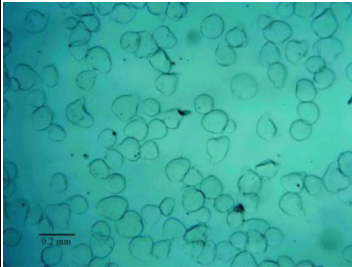
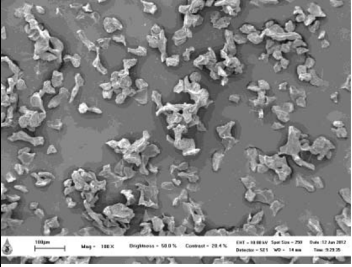
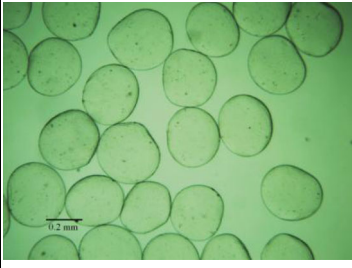
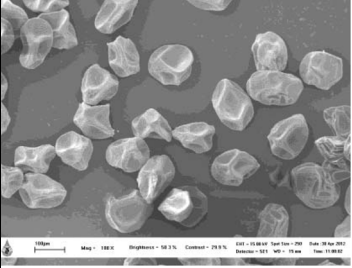
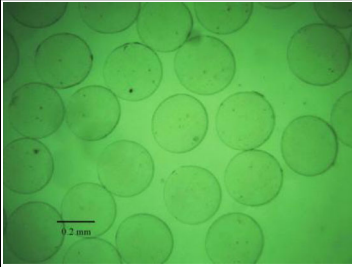
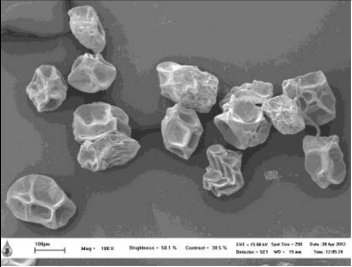
using normal human dermal fibroblasts (NHDF; 7th passage). The ISO 10993-5 standard test method is the test method to assess the *in vitro* cytotoxicity of medical devices. First, the cells were cultured in Dulbecco's modified Eagle's medium (DMEM; Sigma-Aldrich, USA), supplemented by 10% fetal bovine serum (FBS; Invitrogen Corp., USA), 1% L-glutamine (Invitrogen Corp., USA), and 1% antibiotic and antimycotic formulation [containing penicillin G sodium, streptomycin sulfate, and amphotericin B (Invitrogen Corp., USA)]. The genipin-cross-linked gelatin scaffolds that had been cross-linked with 3, 4, 5, and 6% *w/w* of genipin ( $47 \pm 1$  mg) were sterilized by UV radiation for  $\sim 1$  h and then were immersed in 1 mL of serum-free medium (SFM; containing DMEM, 1% L-glutamine, 1% lactalbumin, and 1% antibiotic and antimycotic formulation) for 24 h in incubation to produce extraction media. NHDF cells were separately cultured in wells of TCPS at 10,000 cells/well in serum-containing DMEM for 24 h to allow cell attachment. The cells were then starved with SFM for 24 h. After that, the medium was replaced with an extraction medium and cells were re-incubated for 24 h. The viability of the cells cultured by each of the extraction medium was determined with 3-(4,5-dimethylthiazol-2-yl)-2,5-diphenyltetrazolium bromide (MTT) assay, with the viability of the cells cultured by fresh SFM used as control.

The MTT assay is based on the reduction of the yellow tetrazolium salt to purple formazan crystals by dehydrogenase enzymes secreted from the mitochondria of metabolically active cells. The amount of purple formazan crystals formed is proportional to the number of viable cells. First, each culture medium was aspirated and replaced with 25  $\mu\text{L}$ /well of MTT solution at 5  $\text{mg} \cdot \text{mL}^{-1}$  for a 96-well TCPS. The plate was incubated for 2 h at 37°C. The solution was then aspirated, and 100  $\mu\text{L}$ /well of DMSO was added to dissolve the formazan crystals. After 3 min of rotary agitation, the absorbance at the wavelength of 570 nm representing the viability of the cells was measured using a SpectraMax M2 Microplate Reader.

#### Water Swelling and Weight Loss Behaviors of AgNPs-Loaded Calcium Alginate Beads Embedded in Gelatin Scaffolds

The water swelling and the weight loss behaviors of the AgNPs-loaded calcium alginate beads embedded in gelatin scaffolds were investigated in a phosphate buffer solution (PBS) at the physiological temperature of 37°C for 1, 3, and 5 days. The measurements of each sample were calculated according to the following equations:

**Table I.** Representative OM and SEM Images Illustrating the Effect of the Concentration of the Alginate Solutions on the Morphology of the Obtained Beads at an Applied Voltage of 12 kV/15 cm as Well as the Average Values of Bead Diameters

Alginate solution (% w/v)	Observed by			
	OM	Bead diameters ( $\mu\text{m}$ )	SEM	Bead diameters ( $\mu\text{m}$ )
0.5		$123.19 \pm 17.85$		$39.63 \pm 4.83$
1.0		$306.63 \pm 22.83$		$167.94 \pm 27.23$
1.5		$331.51 \pm 8.70$		$170.11 \pm 21.12$



$$\text{Water swelling(\%)} = \frac{M - M_d}{M_d} \times 100, \quad (1)$$

$$\text{and Weight loss(\%)} = \frac{M_i - M_d}{M_i} \times 100, \quad (2)$$

where  $M$  is the weight of each sample after submersion in a buffer solution for a certain period of time (1, 3, and 5 days),  $M_d$  is the weight of each sample after submersion in the buffer solution for a certain period of time (1, 3, and 5 days) in its dry state, and  $M_i$  is the initial weight of each sample in its dry state.

### Statistical Analysis

Data were presented as means  $\pm$  standard errors of means. Statistical analysis was carried out by the one-way analysis of variance (one-way ANOVA) and Scheffe's post

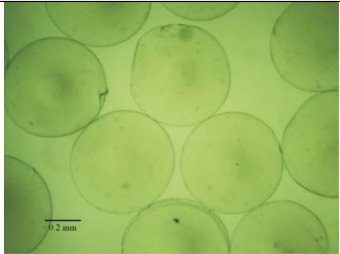
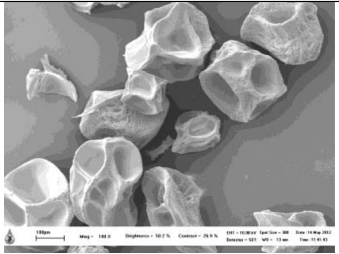
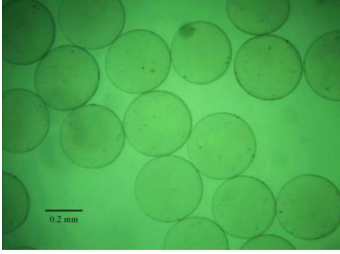
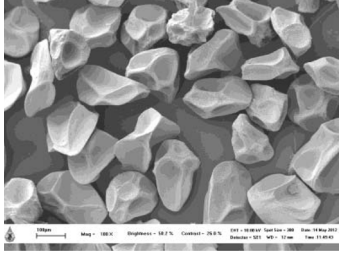
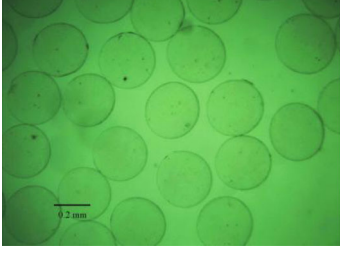
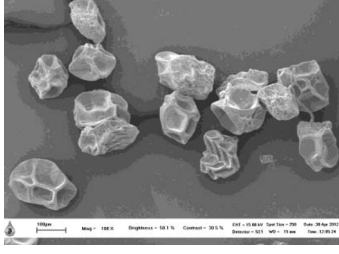
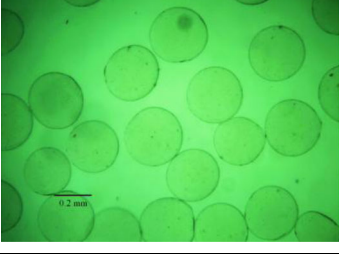
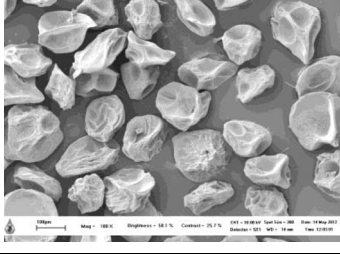
hoc test in SPSS (IBM SPSS, USA). The statistical significance was accepted at  $p < 0.5$ .

## RESULTS AND DISCUSSION

### Neat and AgNPs-Loaded Calcium Alginate Beads

The effect of the concentration of the alginate solutions (*i.e.*, 0.5, 1.0, and 1.5% *w/v*) and the applied voltage (*i.e.*, 8, 10, 12, and 15 kV over a fixed collection distance of 15 cm) on morphology and size of the calcium alginate beads was reported (see Table I in the Supplementary Information). The shapes and diameters of both the wet and dry calcium alginate beads were observed by OM and SEM, respectively. The results are shown in Tables I and II. The results showed that the diameters of all dry calcium alginate beads were smaller than the diameters of the wet calcium alginate beads because

**Table II.** Representative OM and SEM Images Illustrating the Effect of the Applied Voltage on the Morphology of the Obtained Beads at a Fixed Alginate Concentration of 1.5% *w/v* as Well as the Average Values of Bead Diameters

Applied voltage (kV)	Observed by			
	OM	Bead diameters ( $\mu\text{m}$ )	SEM	Bead diameters ( $\mu\text{m}$ )
8		618.83 $\pm$ 17.35		275.96 $\pm$ 41.67
10		383.27 $\pm$ 16.39		193.06 $\pm$ 26.96
12		331.51 $\pm$ 8.70		170.11 $\pm$ 21.12
15		316.02 $\pm$ 20.19		147.72 $\pm$ 17.14

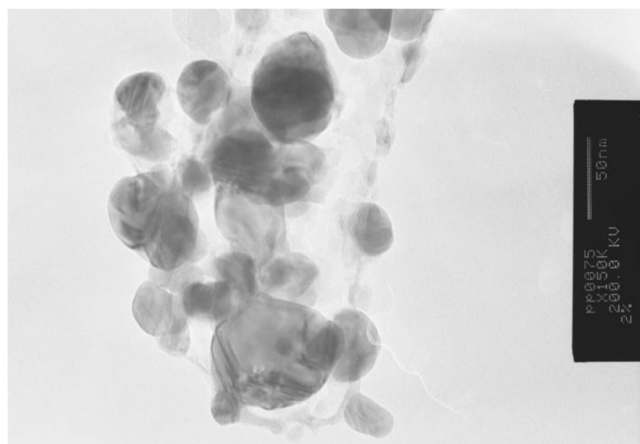


**Fig. 4.** Selected TEM image of the 2% AgNPs-loaded calcium alginate beads

the water molecules in dry beads diffused out from the beads. The effect of the concentration of the alginate solution at the fixed applied voltage of 12 kV on the diameters of beads is also shown in Table I. According to the obtained results, the diameters of the dry calcium alginate beads obtained under these conditions ranged between 40 and 170  $\mu\text{m}$ . For a given applied voltage, increasing concentration of alginate solution caused the diameters of the beads to increase. Moreover, the beads became more spherical when the alginate concentration was increased. The effect of the applied voltage at the fixed alginate concentration of 1.5% *w/v* on the diameters of beads is also shown in Table II. According to this result, the diameters of the dry calcium alginate beads obtained under these conditions ranged between 148 and 276  $\mu\text{m}$ . For a given concentration, increasing the applied voltage caused the diameters of the beads to decrease, except for alginate concentration of 0.5% *w/v* and the applied voltage of 15 kV (see the [supplementary data](#)). The increase of the applied voltage could overcome the surface tension force of the alginate droplet, resulting in the decrease of the bead diameters while the increase of the alginate concentration increased the surface tension force of the alginate droplet, resulting in the increase of the bead diameters. Hence, the factors affecting the diameters and shapes of the calcium alginate beads were the concentration of the alginate solution and the applied voltage. To further investigate the electrospinning of the AgNPs-loaded calcium alginate beads, the alginate concentration of 1.5% *w/v* and the applied voltage of 12 kV over a fixed collection distance of 15 cm were chosen as the model condition. As mentioned, Shi *et al.* (2011) reported that the higher applied voltages could allow the alginate beads to become smaller because the high applied voltage provided the stronger electrical force on the surface of the alginate droplets to small inject formed. The high concentration of the alginate solution was viscous and sticky that affected the solution and could not regurgitate round shape. For the low concentration of the solution, the alginate molecules were not enough on the surface layer. The shrinkage of the bead surface occurred after gelation; thus, the tear-like structure of the beads was observed. The results indicated that the concentration of the alginate solution affected the shape of the beads significantly (8).

According to Tables I and II, the 1.5% *w/v* alginate solution that was electrospun under the fixed applied voltage of 12 kV/15 cm was chosen as the model condition for further investigation.

Because it was easy to spray and the shape of the beads was more spherical. The AgNPs-loaded calcium alginate beads were prepared by adding varying amounts of the  $\text{AgNO}_3$  (*i.e.*, 1, 2, and 3% *w/w* based on the weight of sodium alginate powder) to the 1.5% *w/v* alginate solution. Before electrospinning, the base sodium alginate solutions containing varying amounts of the  $\text{AgNO}_3$  were irradiated by UV irradiation for 1 h. The  $\text{Ag}^+$  ions in the alginate solutions were reduced to AgNPs. After electrospinning, the AgNPs were obtained within the calcium alginate beads as shown in Fig. 4. The shapes and diameters of both the wet and dry AgNPs-loaded calcium alginate beads were observed by OM and SEM, respectively, and the results are shown in Table III. The diameters of the wet 1, 2, and 3% AgNPs-loaded calcium alginate beads were  $573.46 \pm 17.64$ ,  $512.27 \pm 13.13$ , and  $462.86 \pm 12.59$   $\mu\text{m}$ , respectively, while the diameters of the dry 1, 2, and 3% AgNPs-loaded calcium alginate beads were  $171.33 \pm 21.39$ ,  $166.89 \pm 16.65$ , and  $153.71 \pm 15.16$   $\mu\text{m}$ , respectively. From Table III, increasing of the  $\text{AgNO}_3$  concentrations decreased the diameters of the AgNPs-loaded calcium alginate beads. These results could be supported by the shear viscosity and electrical conductivity of the AgNPs-containing alginate solutions, results as shown in Table IV. From Table IV, the shear viscosity of the solutions decreased with increasing  $\text{AgNO}_3$  concentration while the electrical conductivity of the solutions increased with increasing the  $\text{AgNO}_3$  concentration. The increased electrical conductivity of the AgNPs-containing alginate solutions was a direct result of an increase in the amount of  $\text{Ag}^+$  ions within the AgNPs-containing alginate solutions. This increase in the number of charge carriers caused both electrostatic and coulombic repulsive forces to overcome the surface tension of the solutions, leading to the smaller diameters of the beads (8).

#### Genipin-Cross-linked Gelatin Scaffolds and AgNPs-Loaded Calcium Alginate Beads Embedded in Gelatin Scaffolds

Representative SEM images of the gelatin scaffolds prepared from 5% *w/v* of gelatin solution and cross-linked with various concentrations of genipin (*i.e.*, 3, 4, 5, and 6% *w/w* based on the weight of gelatin powder) are shown in Table V. The results showed that the interconnected porous structure of all scaffolds was obtained. The pore size of these scaffolds ranged between  $179.38 \pm 49.68$   $\mu\text{m}$  and  $203.30 \pm 70.93$   $\mu\text{m}$ . In addition, the gelatin scaffolds that had been cross-linked with 5% *w/w* of genipin showed the larger size of interconnected porous structure than other scaffolds. However, increasing the concentration of genipin did not affect the pore size of scaffolds. Tonda-Turo *et al.* (2011) reported that the mean pore size of the pure 2.5% *w/v* of gelatin scaffolds and the gelatin scaffolds cross-linked with genipin was about 140 and 120  $\mu\text{m}$ , respectively (25), while Abbasi *et al.* (2008) reported that the increase of the genipin concentration caused the pore size of gelatin matrices to decrease (26). The representative SEM images of the AgNPs-loaded calcium alginate beads embedded in gelatin scaffolds are shown in Table VI. The results showed that the interconnected porous structure of all scaffolds was obtained. The pore size of these scaffolds ranged between  $154.70 \pm 37.30$   $\mu\text{m}$  and  $245.06 \pm 68.38$   $\mu\text{m}$  while the pore size of the gelatin scaffolds unembedded with the AgNPs-loaded calcium alginate beads was  $179.38 \pm 49.68$   $\mu\text{m}$  (see Table V). However, embedding of the AgNPs-loaded calcium alginate beads into the gelatin scaffolds did not affect the pore size of the scaffolds. To be used as scaffold

materials or wound dressings, the pore size of polymeric scaffolds should facilitate cell seeding, attachment, and also allow liquid flow to transport nutrients through the porosity of materials. Thus, the optimal pore size of scaffolds was in the range between 100 and 500  $\mu\text{m}$  (27).

### Indirect Cytotoxicity Evaluation of Genipin-Cross-linked Gelatin Scaffolds

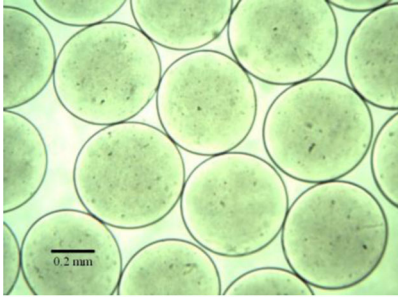
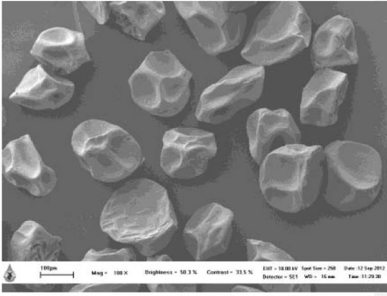
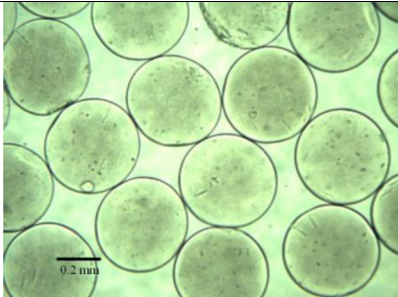
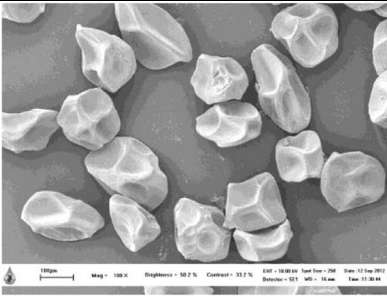
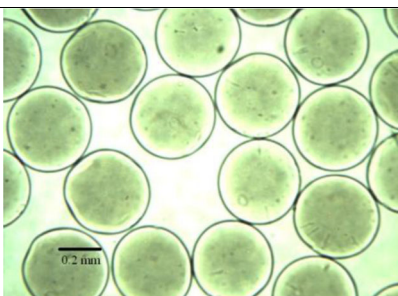
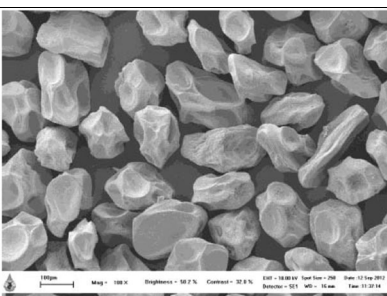
To assess the toxicity of the genipin-cross-linked gelatin scaffolds, indirect cytotoxicity evaluation was carried out. The gelatin scaffolds cross-linked with various genipin concentrations (*i.e.*, 3, 4, 5, and 6% *w/w* based on the weight of gelatin powder) were evaluated for their cytotoxicity. The viability of

the NHDF cultured with the extraction media from these samples in comparison with that of the cells cultured with the fresh culture medium is shown in Fig. 5. Obviously, the viability of the cells cultured with all the extraction media from the genipin-cross-linked gelatin scaffolds with various genipin concentrations ranged between ~85 and ~100%, indicating that all the genipin-cross-linked gelatin scaffolds were proven nontoxic to NHDF, indicating their potential uses for wound dressings.

### Water Swelling and Weight Loss Behaviors of AgNPs-Loaded Calcium Alginate Beads Embedded in Gelatin Scaffolds

The water swelling and the weight loss behaviors of the 1, 2, and 3% AgNPs-loaded calcium alginate beads embedded in

**Table III.** Representative OM and SEM Images of the AgNPs-Loaded Calcium Alginate Beads at Various Concentrations of  $\text{AgNO}_3$

Concentration of $\text{AgNO}_3$ (% <i>w/w</i> )	Observed by	
	OM	SEM
1		
Diameters ( $\mu\text{m}$ )	$573.46 \pm 17.64$	$171.33 \pm 21.39$
2		
Diameters ( $\mu\text{m}$ )	$512.27 \pm 13.13$	$166.89 \pm 16.65$
3		
Diameters ( $\mu\text{m}$ )	$462.86 \pm 12.59$	$153.71 \pm 15.16$

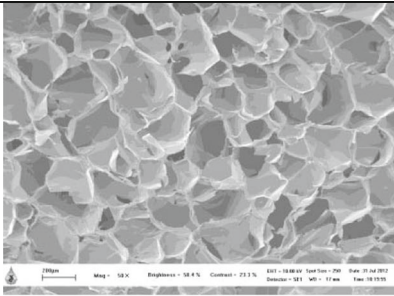
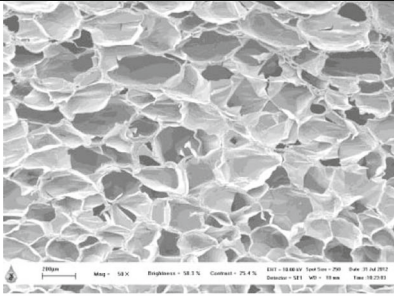
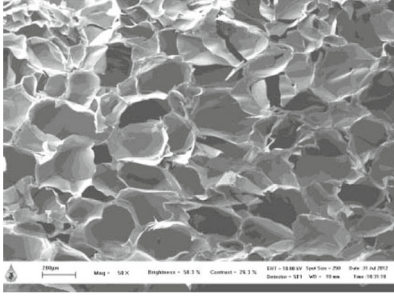
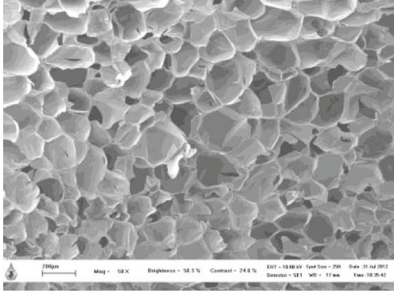


**Table IV.** Shear Viscosity and Electrical Conductivity of the AgNPs-Containing Alginate Solutions at Various Concentrations of AgNO<sub>3</sub> (*n*=3)

Type of alginate solution	Shear viscosity (mPa s)	Electrical conductivity ( $\mu\text{S cm}^{-1}$ )
With 1% AgNO <sub>3</sub> (based on weight of alginate)	96.9±1.2	1,850±12
With 2% AgNO <sub>3</sub> (based on weight of alginate)	96.4±1.6	1,872±20
With 3% AgNO <sub>3</sub> (based on weight of alginate)	90.4±1.4	1,919±13

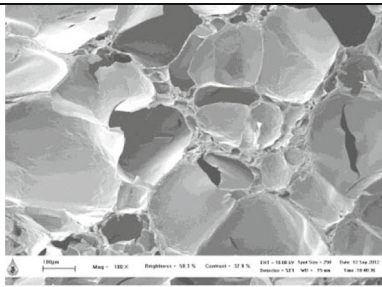
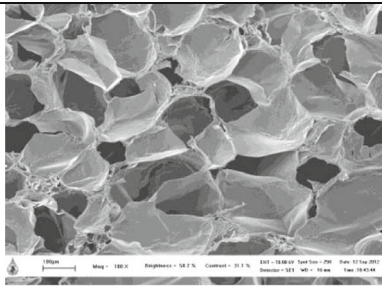
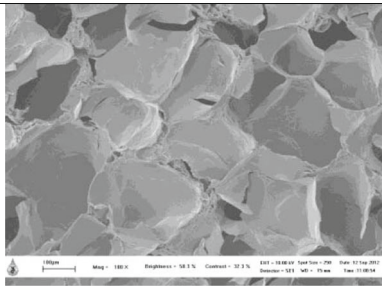
gelatin scaffolds after submersion in PBS at 37°C for 1, 3, and 5 days were investigated, and the results are shown in Fig. 6. At 1 day after submersion in PBS, the water swelling of the 1, 2, and 3% AgNPs-loaded beads embedded in gelatin scaffolds was ~744, ~738, and ~752%, respectively (see Fig. 6a). At 3 days, the value increased to ~805, ~796, and ~802%,

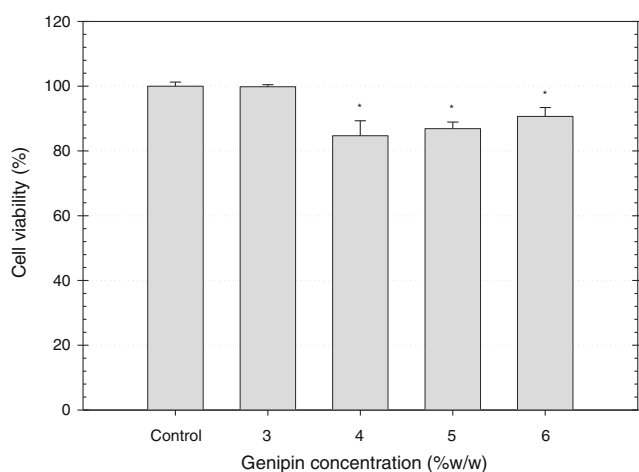
**Table V.** Representative SEM Images of the Genipin-Cross-linked Gelatin Scaffolds with Different Genipin Concentrations as Well as the Average Values of Pore Sizes

Genipin concentration (% w/w, based on weight of gelatin)	Representative SEM images of scaffolds	Pore sizes ( $\mu\text{m}$ )
3		179.38 ± 49.68
4		184.21 ± 59.15
5		203.30 ± 70.93
6		179.60 ± 49.37



**Table VI.** Representative SEM Images of the AgNPs-Loaded Calcium Alginate Beads Embedded in Gelatin Scaffolds as Well as the Average Values of Pore Sizes

Concentration of AgNO <sub>3</sub> (% w/w)	Representative SEM images of scaffolds	Pore sizes (μm)
1		245.06 ± 68.38
2		154.70 ± 37.30
3		184.44 ± 60.20

**Fig. 5.** Indirect cytotoxicity evaluation of genipin-cross-linked gelatin scaffolds with different genipin concentrations after 24 h of cell culture ( $n=3$ ) \* $p<0.05$  compared with control

respectively. At 5 days, the value also increased to ~889, ~909, and ~942%, respectively. Thus, the water swelling of all the AgNPs-loaded calcium alginate beads embedded in gelatin scaffolds increased with increasing submersion time. However, the increasing of AgNO<sub>3</sub> content for loading in the gelatin scaffolds did not much affect the water swelling of these scaffolds.

The weight loss behavior of the AgNPs-loaded calcium alginate beads embedded in gelatin scaffolds after submersion in PBS at 37°C for 1, 3, and 5 days is shown in Fig. 6b. At 1 day after submersion in PBS, the weight loss of the 1, 2, and 3% AgNPs-loaded beads embedded in gelatin scaffolds was ~7, ~8, and ~7%, respectively, while at 3 days, the value was ~8, ~8, and ~8%, respectively. At 5 days, the value significantly increased to ~14, ~15, and ~17%, respectively. Similar to the water swelling behavior, the weight loss of all AgNPs-loaded calcium alginate beads embedded in gelatin scaffolds increased with increasing submersion time, except at day 3, the weight loss of all the AgNPs-loaded calcium alginate beads embedded in gelatin scaffolds was slightly increased. Similarly, the increased AgNO<sub>3</sub> content for loading in the gelatin scaffolds did not much affect the weight loss of these scaffolds.

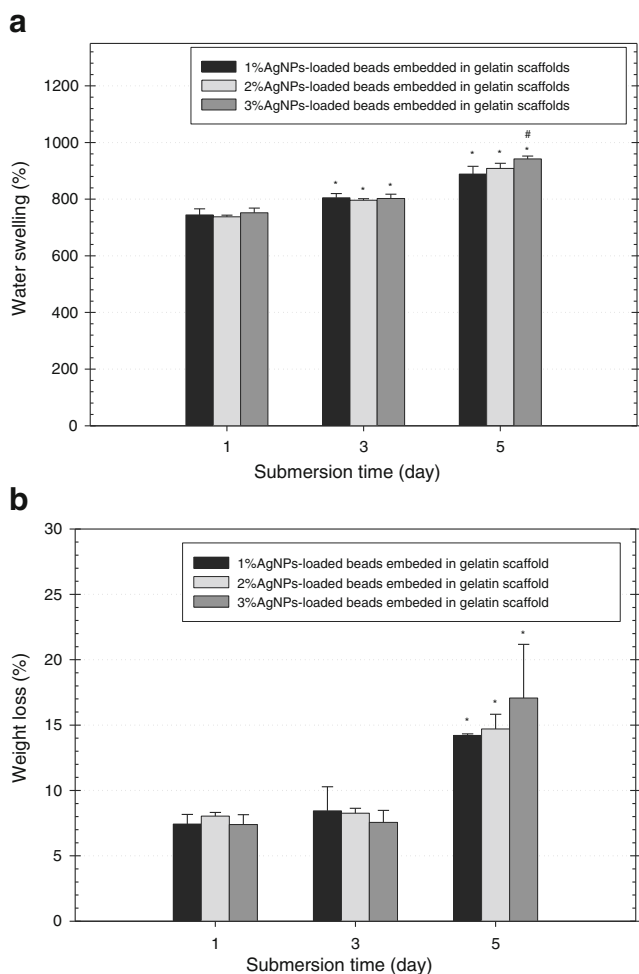


**Fig. 6.** **a** Water swelling and **b** weight loss behaviors of AgNPs-loaded calcium alginate beads embedded in gelatin scaffolds in PBS ( $n=3$ ). \* $p<0.05$  compared with submersion time at day 1 for any given type of sample, and # $p<0.05$  compared with 1% AgNPs-loaded beads embedded in gelatin scaffolds for any given submersion time point

## CONCLUSIONS

In this study, the AgNPs-loaded calcium alginate beads embedded in gelatin scaffolds were successfully prepared. The calcium alginate beads incorporated with AgNPs were obtained by electrospraying method. Factors affecting the shapes and diameters of the calcium alginate beads were the concentration of alginate solution and the applied voltage. Besides, the genipin-cross-linked gelatin scaffolds were proven nontoxic to NHDF, suggesting their potential uses for wound dressings.

## ACKNOWLEDGMENTS

The authors would like to acknowledge the financial support from the Research, Development and Engineering (RD&E) fund through The National Nanotechnology Center (NANOTEC), The National Science and Technology Development Agency (NSTDA), Thailand (P-11-00986) to Mae Fah Luang University (MFU), and Thailand Graduate Institute of Science and Technology (TGIST) (TG-55-99-55-048M).

## REFERENCES

- Sharma VK, Yngard RA, Lin Y. Silver nanoparticles: green synthesis and their antimicrobial activities. *Adv Colloid Interface*. 2009;145:83–96. doi:10.1016/j.cis.2008.09.002.
- Yoksan R, Chirachanchai S. Silver nanoparticles dispersing in chitosan solution: preparation by  $\gamma$ -ray irradiation and their antimicrobial activities. *Mater Chem Phys*. 2009;115:296–302. doi:10.1016/j.matchemphys.2008.12.001.
- Ciach T. Microencapsulation of drugs by electro-hydro-dynamic atomization. *Int J Pharm*. 2006;324:51–5. doi:10.1016/j.ijpharm.2006.06.035.
- Ding L, Lee T, Wang C-H. Fabrication of monodispersed Taxol-loaded particles using electrohydrodynamic atomization. *J Control Release*. 2005;102:395–413. doi:10.1016/j.jconrel.2004.10.011.
- Xie J, Lim LK, Phua Y, Hua J, Wang C-H. Electrohydrodynamic atomization for biodegradable polymeric particle production. *J Colloid Interface Sci*. 2006;302:103–12. doi:10.1016/j.jcis.2006.06.037.
- Cloupeau M. Recipes for use of EHD spraying in cone-jet mode and notes on corona discharge effects. *J Aerosol Sci*. 1994;25:1143–57. doi:10.1016/0021-8502(94)90206-2.
- Jaworek A, Sobczyk AT. Electrospraying route to nanotechnology: an overview. *J Electrostat*. 2008;66:197–219. doi:10.1016/j.elstat.2007.10.001.
- Shi P, He P, Teh TKH, Morsi YS, Goh JCH. Parametric analysis of shape changes of alginate beads. *Powder Technol*. 2011;210:60–6. doi:10.1016/j.powtec.2011.02.023.
- Suksamran T, Opanasopit P, Rojanarata T, Ngawhirunpat T, Ruktanonchai U, Supaphol P. Biodegradable alginate microparticles developed by electrohydrodynamic spraying techniques for oral delivery of protein. *J Microencapsul*. 2009;26:563–70. doi:10.3109/02652040802500622.
- Augst AD, Kong HJ, Mooney DJ. Alginate hydrogels as biomaterials. *Macromol Biosci*. 2006;6:623–33. doi:10.1002/mabi.200600069.
- Martinez CJ, Kim JW, Ye C, Ortiz I, Rowat AC, Marquez M, *et al.* A microfluidic approach to encapsulate living cells in uniform alginate hydrogel microparticles. *Macromol Biosci*. 2012;12:946–51. doi:10.1002/mabi.201100351.
- Thu H-E, Zulfakar MH, Ng S-F. Alginate based bilayer hydrocolloid films as potential slow-release modern wound dressing. *Int J Pharm*. 2012;434:375–83. doi:10.1016/j.ijpharm.2012.05.044.
- Rebelatto MC, Guimond P, Bowersock TL, HogenEsch H. Induction of systemic and mucosal immune response in cattle by intranasal administration of pig serum albumin in alginate microparticles. *Vet Immunol Immunopathol*. 2011;83:93–105. doi:10.1016/S0165-2427(01)00370-1.
- Ouwerx C, Velings N, Mestdagh MM, Axelos MAV. Physicochemical properties and rheology of alginate gel beads formed with various divalent cations. *Polym Gels Netw*. 1998;6:393–408. doi:10.1016/S0966-7822(98)00035-5.
- Rousseau I, Le Cerf D, Picton L, Argillier JF, Muller G. Entrapment and release of sodium polystyrene sulfonate (SPS) from calcium alginate gel beads. *Eur Polym J*. 2004;40:2709–15. doi:10.1016/j.eurpolymj.2004.07.022.
- Chen G, Ushida T, Tateishi T. Scaffold design for tissue engineering. *Macromol Biosci*. 2002;2:67–77. doi:10.1002/1616-5195(20020201)2:2<67::AID-MAB167>3.0.CO;2-F.
- Yarlagadda PK, Chandrasekharan M, Shyan JY. Recent advances and current developments in tissue scaffolding. *Biomed Mater Eng*. 2005;15:159–77.
- Freed LE, Vunjak-Novakovic G, Biron RJ, Eaqls DB, Lesnoy DC, Barlow SK, *et al.* Biodegradable polymer scaffolds for tissue engineering. *Biotechnology*. 1994;12:689–93. doi:10.1038/nbt0794-689.
- Hutmacher DW. Scaffold design and fabrication technologies for engineering tissues—state of the art and future perspectives. *J Biomater Sci Polym Ed*. 2001;12:107–24. doi:10.1163/156856201744489.
- Ma PX, Choi J-W. Biodegradable polymer scaffolds with well-defined interconnected spherical pore network. *Tissue Eng*. 2001;7:23–33. doi:10.1089/107632701300003269.

21. Kang HW, Tabata Y, Ikada Y. Fabrication of porous gelatin scaffolds for tissue engineering. *Biomaterials*. 1999;20:1339–44. doi:10.1016/S0142-9612(99)00036-8.
22. Kim SE, Heo DN, Lee JB, Kim JR, Park SH, Jeon SH, *et al.* Electrospun gelatin/polyurethane blended nanofibers for wound healing. *Biomed Mater*. 2009;4:044106. doi:10.1088/1748-6041/4/4/044106.
23. Darroudi M, Ahmad MB, Zak AK, Zamiri R, Hakimi M. Fabrication and characterization of gelatin stabilized silver nanoparticles under UV-light. *Int J Mol Sci*. 2011;12:6346–56. doi:10.3390/ijms12096346.
24. Chang Y, Tsai CC, Liang HC, Sung HW. Reconstruction of the right ventricular outflow tract with a bovine jugular vein graft fixed with a naturally occurring crosslinking agent (genipin) in a canine model. *J Thorac Cardiovasc Surg*. 2001;122:1208–18. doi:10.1067/mtc.2001.117624.
25. Tonda-Turo C, Gentile P, Saracino S, Chiono V, Nandagiri VK, Muzio G, *et al.* Comparative analysis of gelatin scaffolds crosslinked by genipin and silane coupling agent. *Int J Biol Macromol*. 2011;49:700–6. doi:10.1016/j.ijbiomac.2011.07.002.
26. Abbasi A, Eslamian M, Heyd D, Rousseau D. Controlled release of DSBP from genipin-crosslinked gelatin thin films. *Pharm Dev Technol*. 2008;13:549–57. doi:10.1080/10837450802309679.
27. Ikada Y. Challenges in tissue engineering. *J R Soc Interface*. 2006;3:589–601. doi:10.1098/rsif.2006.0124.